China Ocean Eng., 2018, Vol. 32, No. 4, P. 431–442
DOI: https://doi.org/10.1007/s13344-018-0045-6, ISSN 0890-5487
http://www.chinaoceanengin.cn/ E-mail: coe@nhri.cn

Experimental and Numerical Investigations of Ship Parametric Rolling in Regular Head Waves

MA Shan, GE Wen-peng, R.C. Ertekin, HE Qiang, DUAN Wen-yang*

College of Shipbuilding Engineering, Harbin Engineering University, Harbin 150001, China

Received November 9, 2017; revised April 16, 2018; accepted May 22, 2018

Abstract

Parametric rolling is one of five types of the ship stability failure modes as proposed by IMO. The periodic change of the metacentric height is often considered as the internal cause of this phenomenon. Parametric rolling is a complex nonlinear hydrodynamic problem, often accompanied by large amplitude vertical motions of ships. In recent years, the Reynolds-averaged Navier–Stokes (RANS) equation simulations for viscous flows have made great progress in the field of ship seakeeping. In this paper, the parametric rolling for the C11 containership in regular waves is studied both experimentally and numerically. In the experiments, parametric rolling amplitudes at different drafts, forward speeds and wave steepnesses are analyzed. The differences in the steady amplitudes of parametric rolling are observed for two drafts. The effect of the incident wave steepness (or wave amplitude) is also studied, and this supports previous results obtained on limits of the stability for parametric rolling. In numerical simulations, the ship motions of parametric rolling are analyzed by use of the potential-flow and viscous-flow methods. In the viscous-flow method, the Reynolds-averaged Navier–Stokes equations are solved using the overset grid method. The numerical accuracies of the two methods at different wave steepnesses are also discussed.

Key words: parametric rolling, nonlinear strip theory, CFD method, overset grid method

Citation: Ma, S., Ge, W. P., Ertekin, R. C., He, Q., Duan, W. Y., 2018. Experimental and numerical investigations of ship parametric rolling in regular head waves. China Ocean Eng., 32(4): 431–442, doi: https://doi.org/10.1007/s13344-018-0045-6

1 Introduction

Container ships typically have large decks and relatively pronounced flare bows and sterns. When the ship is travelling in head waves, the parametric roll motion response may happen under some wave conditions. When a slight rolling happens, the ship rolling angle would increase largely after several periods, accompanied by severe heave and pitch, and these may cause the ship to capsize. The phenomenon of the parametric rolling becomes a real threat for the shipping community since a post-Panamax C11 class containership suffered heavy parametric rolling in 1998 (Hashimoto and Umeda, 2004).

The existing methods of the motion prediction can be roughly divided into two categories. One method is based on the potential-flow theory and another is based on the RANS equations. Bulian (2006) established a model with 1.5 degrees of freedom to simulate the parametric rolling in regular/irregular waves, where the parametric roll motion is modeled using a single degree-of-freedom. The additional half degree is meant to consider the influence of free sinkage and trim due to the quasi-static assumption. Lu et al. (2012a) investigated the parametric rolling motion in random waves through the numerical simulations and experiments, and verified the non-ergodic characteristics of the parametric rolling motion in random waves. Liu and Papanikolaou (2016) used a 3-D nonlinear time-domain simulation method to investigate the parametric rolling of the ITTC A1 containership. In the numerical model, the impulse response function concept is applied, where the nonlinear Froude-Krylov/restoring forces are estimated over the actual wetted surface of the ship. Zhou et al. (2016) performed a study of the hybrid prediction method for the parametric rolling. The roll damping estimation is carried out using the viscous-flow CFD approach and the parametric rolling motions are solved using the 3-DOF potential method. Hu et al. (2017) proposed a consistent nonlinear strip theory to predict the parametric rolling for the C11 containership in regular waves.

The viscous-flow based CFD method has provided a new way to solve strongly nonlinear interactions between ships and waves. Simonsen et al. (2013) adopted the URANS code CFDSHIP-IOWA and Star-CCM+ to study the

Foundation item: The present work is financially supported by the National Natural Science Foundation of China (Grant Nos. 51379045, 51679043, and 51679053) and the National Defense Basic Scientific Research Foundation (Grant No. B2420132001).

*Corresponding author. E-mail: duanwenyang@hrbeu.edu.cn

ship response for the KCS container ship in regular head seas. Tezdogan et al. (2015) performed an unsteady RANS simulation to predict the ship motions and the added resistance of a full scale KRISO containership model (KCS) in head waves at a slow steaming speed. The results are compared by use of the potential theory and are found to be in good agreement with the experiments. Castiglione et al. (2011) used the overset grid method for simulating the Delta372 type ship's motion response and wave added resistance at different speeds and for different wave steepnesses. Galbraith and Boulougouris (2015) used the overset grid method to simulate the parametric rolling response of an ONR tumblehome model 5613 in head seas based on the STAR-CCM+ software. During the simulations, the parametric rolling was detected successfully at a given wave period and forward speed, but the numerical simulations are not validated with experimental data. The study proved that the CFD can be a valuable tool for investigating this interesting and complex phenomenon.

Owing to the complexity of the parametric rolling, the model tests have been conducted on the investigation of this phenomenon. Bulian et al. (2008) conducted an experimental study on the parametrically excited rolling motion on a partially restrained post-Panamax containership in head irregular seas. The authors argued that the accurate experimental investigation for the parametric rolling in random seas is not easy and the development of numerical tools is useful to have a more reliable estimation of rolling. Kim et al. (2011) performed a parametric rolling experiment on a cruise ship under bichromatic wave conditions. Via the observation, the occurrence of the parametric rolling in a bichromatic wave is found. Thomas et al. (2008) conducted a parametric rolling test on a twin-propeller containership, and the influence of wave conditions (wave height and wave length), ship speed and transverse metacentric height (GM) on the threshold boundaries of parametric roll behavior is studied.

Lu et al. (2016) conducted the experimental and numerical studies on the effect of parametric rolling on the added resistance in regular head seas in the case of a C11 containership. Lu et al. (2017) studied several elements required for modeling the parametric rolling in head seas by performing free running model experiments. During the parametric rolling experiments, it was interesting to see that there are sub-harmonic components for the pitch and heave motions.

In this paper, the results of both the experimental and numerical studies that we have conducted are given for the parametric rolling phenomenon of the C11 containership in regular waves. In the experiments, two sets of the experiments for different forward speeds and wave steepnesses are tested. The first set of the experiments are done and introduced by Lu et al. (2012b). The second set of the experiments are done in 2016 and briefly introduced by Hu et al. (2017). The drafts used in these two experiments have a 0.3 m difference. Via the comparison of the steady parametric roll amplitude under the same forward speed and wave conditions, the differences in the roll amplitudes can be clearly seen. To have a better understanding on how the differences originate, the restoring rolling moments in waves are analyzed here using the captive model test data. Furthermore, the parametric rolling for relatively large wave steepnesses has been observed in the model tests. The variation of the steady roll amplitude at different wave steepnesses is discussed here based on the previous analytical findings of Neves and Rodríguez (2007). The numerical simulation of the parametric rolling is performed using the CFD method and potential-flow theory. The numerical accuracies of different methods are verified via the comparison with the experimental data. It is found that at a relatively small wave steepness, both the potential-flow theory and CFD method can give quite good results, while the CFD method evidently presents better agreement with the experimental data when compared with the potential-flow method of relatively large wave steepnesses.

2 Experimental measurement of the parametric rolling for C11 containership

The post-Panamax C11 container ship, which is sensitive to the parametric rolling is selected as the ship model used in the experiments. The primary particulars of the ships with the scale factor 1:65.5 are presented in Table 1. The experiments are performed at the seakeeping basin of

Table 1 Main dimension of C11 container ship

Main dimension	Full scale loading case 1	Model scale loading case 1	Full scale loading case 2	Model scale loading case 2
Lpp L (m)	262.0	4.0	262.0	4.0
Breadth B (m)	40.0	0.6107	40.0	0.6107
Depth D (m)	24.45	0.3733	24.45	0.3733
Draft T (m)	11.50	0.1756	11.80	0.1802
Displacement (kg)	6.75×10^7	240.23	6.86×10^7	248.95
KG (m)	18.44	0.2815	18.44	0.2815
X_g (m)	125.52	1.9163	125.23	0.0881
GM (m)	1.928	0.0294	1.900	0.0290
Rolling inertia radius R_{xx} (m)	15.4463	0.2358	15.3859	0.2349
Pitching inertia radius R_{yy} (m)	63.6529	0.9718	62.8800	0.9600

China Ship Science Research Center (CSSRC). In the experimental study, two experiments with different drafts are conducted. The first set of experiments is discussed by Lu et al. (2012b), for the mean draft of 11.5 m. The second set of experiments is conducted in 2016 with a different draft of 11.8 m and is briefly introduced by Hu et al. (2017). In these two sets of experiments, the free running experiments are conducted, and the focus is the parametric rolling measurements in regular waves at different forward speeds and wave steepnesses. The wave length is chosen equal to the ship length. In both experiments, the prototype ship forward speeds of 0, 5, 10 and 15 knots, and correspondingly, the wave steepnesses 0.01, 0.02, 0.03 and 0.04 are used. While in the second set of experiments, the model tests for additional relatively large wave steepnesses of 0.05, 0.06, and 0.07 were conducted in order to study the parametric rolling characteristics of the ship for relatively large wave steepnesses. During the experiments for the parametric rolling and for the case of draft of 11.8 m, the restoring rolling moment in regular waves was also measured. In the measurements of the restoring rolling moment, the ship model is partially constrained using a recently designed device. Via this device, the ship is fixed to a certain heeling angle and the hydrodynamic rolling moment in waves is measured, while keeping the model free in its heave and pitch motions. For further details of the equipment used, the readers can refer to Lu et al. (2017).

In Figs. 1 and 2, the steady roll amplitudes of the ship at different length Froude numbers are presented for the wave steepness H/λ of 0.01, 0.02, 0.03, and 0.04, respectively. From the results, it is seen that the maximum parametric roll motions occur at Fn=0.05. The ship model encounter frequencies with different Froude numbers are 3.93, 4.42, 4.91, and 5.40 rad/s, respectively. The natural roll frequency for the ship with 11.5 m is about 2.11 rad/s. The ship encounter frequency is about two times the roll natural frequency when the Froude number is 0.05. That is the reason why the ship parametric rolling reaches the maximum amplitude at that Froude number. The ship rolling amplitude is the largest under that condition. The steady roll amplitude increases with wave steepness. It is also interesting to observe that the steady parametric rolling amplitude for the draft T=11.5 m is generally larger than that for the draft of 11.8 m.

It is seen from Table 1 that the principle particulars under these two draft conditions, like the metacentric height GM and roll inertia radius, are quite close. The parametric rolling is due physically to the periodical change of the restoring moment in waves. Therefore, to analyze the causes of different parametric rolling amplitudes in these two draft cases, the following analysis has to be made.

In head seas, there is significant coupling between the heave, pitch and roll motions (Lu et al., 2012b). Based on the mathematical analysis of the parametric excitation by Neves and Rodríguez (2006), the restoring arm variation of a ship in waves not only depends on the incident wave, but also on the heave and pitch motions. To investigate which factor leads to the differences of the parametric rolling for ship models of different drafts, the experimental restoring moments in waves at a fixed heeling angle (with free heave

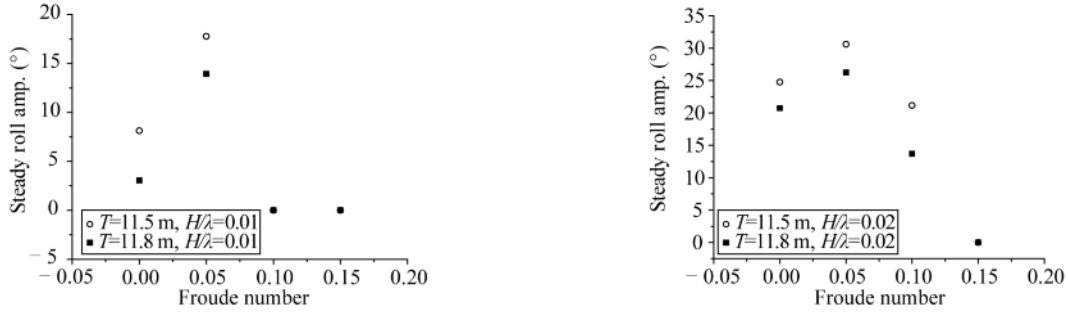

Fig. 1. Comparison of steady roll amplitudes under the incident wave steepnesses H/λ=0.01, 0.02 in two different draft cases.

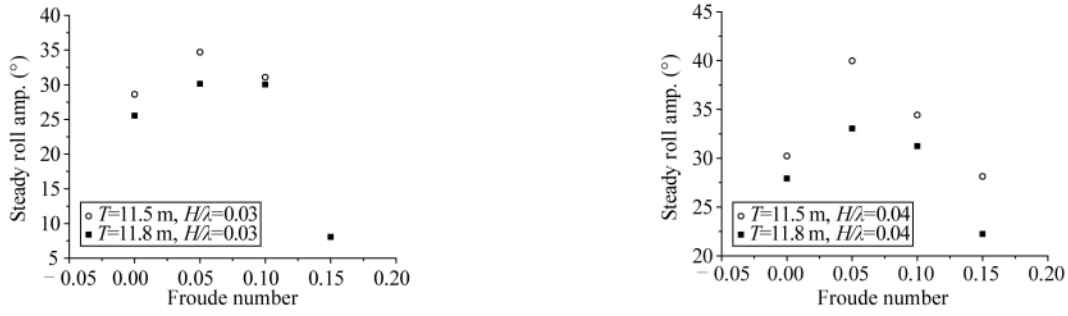

Fig. 2. Comparison of steady roll amplitudes under the incident wave steepnesses H/λ=0.03, 0.04 in two different draft cases.

and pitch motions) are compared for the ship models of different drafts.

Fig. 3 compares the variation of the metacentric height (GM) for different forward speeds for the incident wave steepness H/λ of 0.02 for the two draft cases. Gu et al. (2014) and Lu et al. (2016) provided the experimental righting arm GZ curves for the ship model with the draft of 11.5 m. During the restoring moment experiments, the fixed heeling angles in the two draft cases are slightly different. For the ship model with the draft of 11.5 m, the restrained heeling angle is about 7.3°, while it is 7.7° for the ship model with 11.8 m draft. In Fig. 3, the restoring GZ curves have been converted to the GM variation curves here for the convenience of comparison.

From Fig. 3, it is seen that the differences for the *GM* variation are not clear at zero forward speed; they become more evident as the forward speed increases. To better illustrate the difference of the restoring moment *GM* variation curves of the two drafts, Table 2 presents the typical parameters related to *GM* in waves estimated from the *GM* curves in Fig. 3. In Table 2, GM_{mean} and GM_{amp} are the mean and amplitude of the *GM* variation in regular waves, respectively, GM_{amp}/GM_{mean} represents the variation of GM_{amp} relative to the mean value in waves, and it reflects the extent of the vulnerability to the parametric rolling stability failure mode (International Maritime Organization, 2015, 2016).

At the forward speeds Fn=0.05, 0.10, it is seen that GM_{amp} and relative variation amplitude GM_{amp}/GM_{mean} in the case of the draft of 11.5 m are obviously larger than those of the case of 11.8 m draft. This comparison could explain why the steady roll amplitudes of the parametric rolling at 11.5 m draft are greater than those of 11.8 m draft shown in Fig. 1 (incident wave steepness 0.02, Fn=0.05, 0.10). At forward speed of Fn=0.15, it can be seen that both GM_{mean} and GM_{amp} for the 11.5 m draft case are larger than that for the 11.8 draft case. In Fig. 1, the parametric rolling did not occur for the case of 11.5 m draft, and the parametric rolling motion remains quite small for the case of 11.8 m draft. It is concluded that this is due to the relatively larger value of average GM_{mean} in waves for the 11.5 m case, which contributes to larger stability in waves, and the ship model does not experience the parametric rolling in waves.

At the zero forward-speed, the variation amplitude GM_{amp} and mean value GM_{mean} for the two draft cases are quite close to each other as shown in Table 2. It is seen in

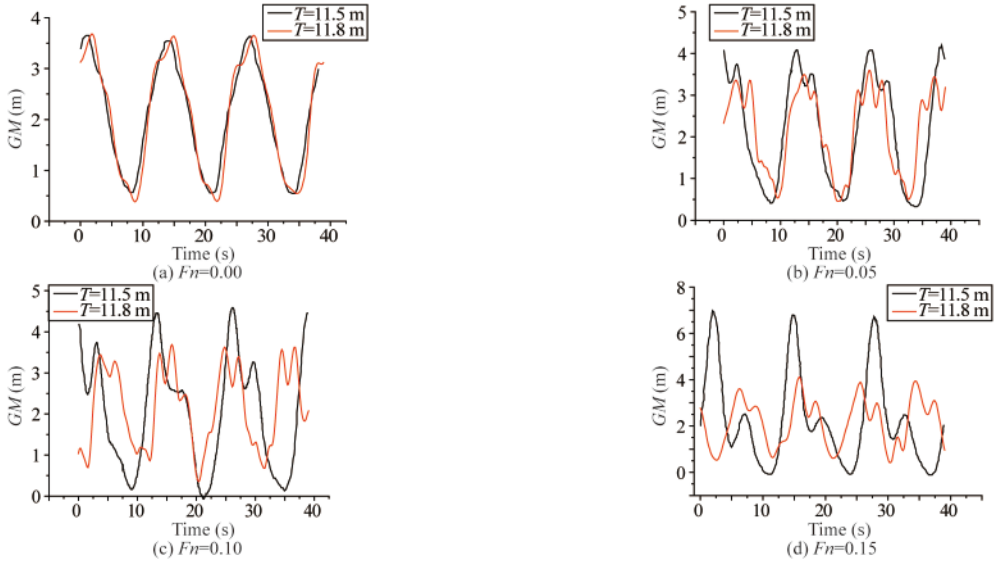

Fig. 3. Comparison of the GM variation curve at different forward speeds in two different draft cases (the incident wave steepness is 0.02).

Table 2 Parameters for the GM curves in waves for the ship models in two draft cases

Fn	Full scale draft (m)	Model draft (m)	GM_0 in calm water (m)	GM_{mean} in regular wave (m)	GM_{amp} in regular wave (m)	GM_{amp}/GM_{mean}
0.00	11.5	0.1756	1.926	2.050	1.493	0.7282
	11.8	0.1802	1.900	2.011	1.618	0.8066
0.05	11.5	0.1756	1.926	2.234	1.841	0.8218
	11.8	0.1802	1.900	2.024	1.480	0.7314
0.10	11.5	0.1756	1.926	2.332	2.129	0.9138
	11.8	0.1802	1.900	2.273	1.421	0.6251
0.15	11.5	0.1756	1.926	3.347	3.432	1.0250
	11.8	0.1802	1.900	2.378	1.729	0.7278

Fig. 1 that the steady parametric roll amplitude for the 11.5 m case is slightly larger than that for the 11.8 m case. The current comparison from the GM variation in waves cannot fully explain the reason for different steady rolling amplitudes. Further analysis is needed for better understanding of the differences of the response in two different draft cases and in zero forward-speed case.

Fig. 4 shows the body plan for the C11 containership. The waterlines for 11.5 m and 11.8 ship models are also given. It can be seen that there are several aft stations from #0 to #1.5, whose half breadth changes very abruptly around the waterlines. Especially, the change of the waterline breadth at the #1 station from 11.5 m to 11.8 m is evident. The large change of the half breadth close to the waterline generally causes a more violent variation of the parametric excitation for the ship model with 11.5 m draft. From the observation of the present model test results, it is concluded that the draft at aft stations has quite significant influence on the inception of the parametric rolling of the C11 containership. The aft draft can be changed by adjusting the trim of the ship in the marine service. In the ship design phase, the optimization of the aft body plan is also possible to reduce the amplitude of the parametric rolling in waves.

In the experiments, the parametric rolling tests at relatively large wave steepnesses of 0.05, 0.06, and 0.07 are also conducted for the 11.8 m draft model. Fig. 5 shows the steady parametric rolling amplitude that varies with the wave steepness at Fn=0.05, 0.1. From the results, it is interesting to see that the roll amplitude increases with the wave

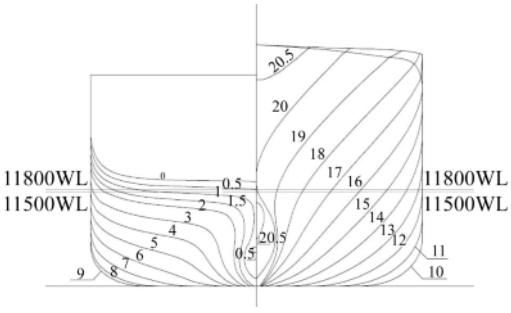

Fig. 4. Body plan for the C11 containership.

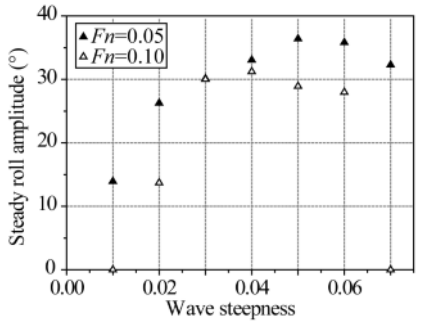

Fig. 5. Steady parametric roll amplitude variation as a function of the wave steepness at two different forward speeds.

height firstly and then it decreases at a certain wave height. This means that the ship rolling amplitude will not always increase with the wave height. Neves and Rodríguez (2007) analyzed analytically the unstable region for the parametric rolling. They found that there are additional nonlinear and non-oscillatory restoring stiffness (hardening effect on the dynamic system) which is proportional to the wave amplitude square. This additional term will make the percentage of the change of the restoring moment with respect to the calm water restoring moment smaller, thus reducing the sensitivity of the ship dynamics to the parametric rolling. Based on their discussion, the parametric excitation and possibly the parametric rolling amplitude will be reduced with the increase of the additional stiffness above a certain level of the wave amplitude at a certain frequency. Their mathematical model is definitely helpful to understand this complex dynamics of the parametric rolling.

In this paper, the parametric rolling experiments in the relatively large range of wave steepnesses are carried out. As shown in Fig. 5, the amplitude of the parametric rolling is surely reduced at certain wave amplitude which supports the analysis of Neves and Rodríguez (2007). Furthermore, the experimental data provide a direct indication of the parametric rolling characteristics for larger wave heights for this ship model and help to give quantifiable results due to the hardening effect of the restoring moment.

3 Potential-flow based nonlinear strip theory to predict parametric rolling

In this paper, both the CFD and potential-flow model are used to simulate the parametric rolling in waves. The potential-flow model used here is based on the nonlinear strip theory. In this model, the radiation and diffraction fluid forces are calculated by using the linear impulse response function method; the hydrodynamic coefficients in the time domain are obtained from the Fourier transformation of the hydrodynamic coefficients in the frequency domain by the strip theory. In the numerical calculation of the radiation forces in the time domain, the consistent treatment of the impulse response functions has already been formulated; and the related theoretical analysis can be found in Ma et al. (2016). To model the restoring arm variation in waves, the Froude-Krylov forces and hydrostatic forces are estimated on the wetted hull-surface under the instantaneous wave surface. The parametric roll motions are solved together with the dynamic heave and pitch motions for the purpose of including the coupling effect of the heave/pitch motions. For further details of the theoretical modelling, the reader can refer to the work of Hu et al. (2017).

4 CFD modelling to predict the parametric rolling

4.1 Controlling equations

In the present study, the commercial software Star-CCM+ is applied to perform the parametric rolling simula-

tion for the C11 containership. In the numerical simulations, the viscous flow is modeled by using the incompressible, unsteady Reynolds-averaged Navier–Stokes equations (RANS) (see e.g., Tezdogan et al., 2015).

The finite-volume method is used to discretize the integral formulation of the Navier–Stokes equations, where the convective term is adopted to the second-order upwind scheme. The position of the free surface between the water and the air is modeled by using the Volume of Fluid (VOF) method. The turbulence model selected in this paper is the SST k–ω turbulence model.

4.2 Investigation of the wave generation in a numerical wave tank

Before performing the numerical simulations of the ship motion in waves, the incident wave generation has to be studied to obtain high quality incident waves. To establish a numerical wave tank, the wave-making and wave-eliminating sources are necessary in the physical tank. The numerical wave tank set up is shown in Fig. 6. The wave tank covers 10 wave lengths. The damping zones are divided into two levels, where the grid size in Damping zone 2 is larger than that of Damping zone 1 to accelerate the numerical dissipation of wave energy.

The wave dissipation will occur during the wave propagation. One cause of the dissipation is due to the fluid viscosity. Another reason is due to the numerical dissipation; and the potentially improper grid discretization contributes to this. The numerical dissipation does accumulate along the wave propagation and it deteriorates the physical waves. In this paper, the influence of the number of grids on the wave is studied through the Courant number $C=U\Delta t/\Delta x$ smaller than 1 (U is the wave celerity, Δt is the time step and Δx is the minimum grid cell size).

In the numerical wave generation, the linear Airy wave model is used. The generated regular wave, with the wave length of 4.0 m and wave height of 0.12 m is considered to be correlated to the analytical model. In the horizontal direction, the grid is evenly distributed. In the vertical direction, however, the grid is evenly distributed within one wave height range across the calm water surface, and it gradually becomes sparse away from the wave surface. In the grid discretization study, N_x represents the number of the grid cell within one wave length horizontally, while N_y represents the number of grid cells in one wave height vertically near the free surface. The different settings of the grid number in the horizontal/vertical direction are shown in Table 3, where A,

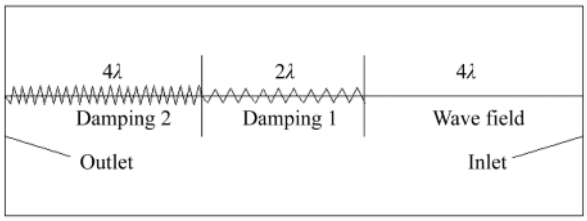

Fig. 6. Schematic diagram of the numerical wave tank.

Table 3 Horizontal and vertical combinations of different grid numbers of the numerical wave tank

Mesh discretization settings	A (N_y–N_x)	B (N_y–N_x)	C (N_y–N_x)
I (N_y–N_x)	8–66	16–66	32–66
II (N_y–N_x)	10–80	20–80	38–80
III (N_y–N_x)	12–100	24–100	48–100
IV (N_y–N_x)	16–133	32–133	64–133

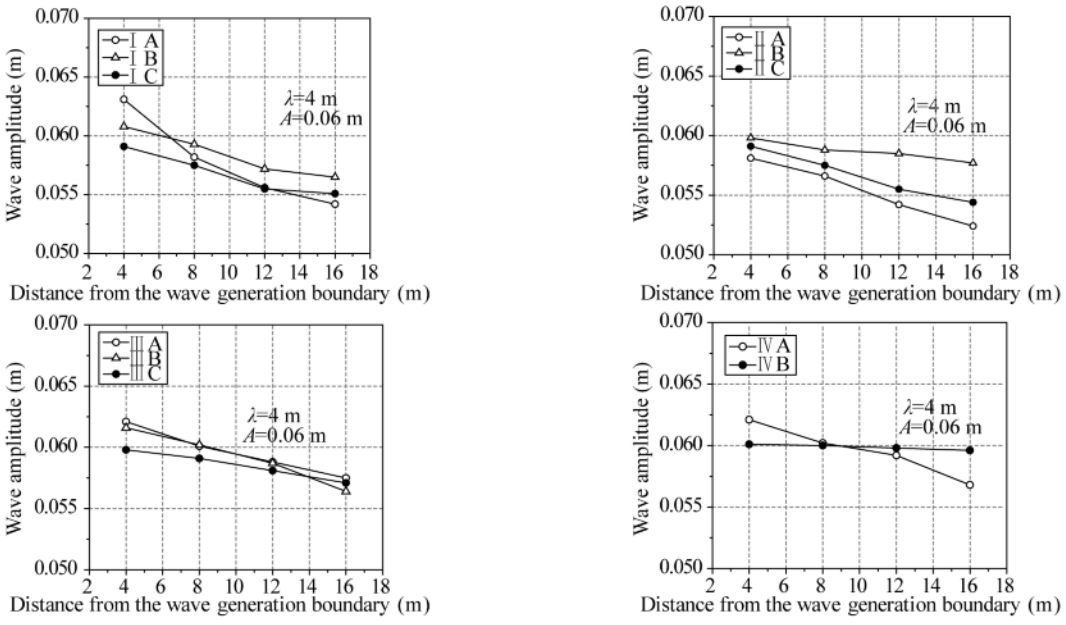

Fig. 7. Variation of the generated wave amplitude at different longitudinal locations.

B, C represent the settings at different columns and I, II, III, IV represent the settings at different rows, respectively.

Fig. 7 shows the wave-amplitude distribution along the wave propagation direction when the generated wave reaches a steady state. Since the grid number for the IVC configuration is very large, the wave simulation is not performed. It is seen from Fig. 7 that the generated wave amplitude becomes steadier and gets closer to the target value in general with the refinement of the longitudinal grid N_x. When N_x increases to 100, the average amplitude of the wave surface reaches 0.0598 m, which is quite close to the target wave amplitude. As the vertical grid number N_y increases, the generated steady wave amplitude tends to increase and then it decreases again which can be found more evident from the first two subplots in Fig. 7. When N_y is about 20 grids in the IIB grid configuration, the amplitude is quite close to the target wave amplitude. In addition, the average of the generated wave amplitudes at four wave gauges of the IIB wave is 0.0587 m. By taking into account the impact of the grid size on the computational time, the IIB grid configuration is used in the CFD simulation of the parametric rolling for the C11 containership.

4.3 Geometrical model

Fig. 8 shows the established geometry of the model. During the experimental and CFD studies, the bilge keel is included, with its length of 76.54 m and width of 0.4 m in full scale. The bilge keel is located at both sides of the amidship.

4.4 Computational domain selection and boundary conditions

The choice of the computational domain has great influence on the accuracy of the simulations. The whole domain is divided into the incident wave zone, wake flow zone and damping dissipation zone along the wave propagation direction. The selection of the incident wave region considers the development of the incident wave and the effect of the hull boundary on the wave reflection, as shown in Fig. 9, with λ being the wave length. The phenomenon of the flow separation exists at the stern of the ship, and it has a great influence on the motion of the ship, but the effect becomes weak when the wake flow zone moves away with the wave, and thus the grid with variable sizes is used in the wake region. The damping zone is far away from the hull but near the outlet of the flow field, thus, sparse grid is adopted there.

The setting of the boundary conditions is very important when the viscous CFD simulations are done. In the present study, the boundary conditions used are from the study of Tezdogan et al. (2015). The horizontal inlet and the top and bottom of the domain are the velocity inlets, the horizontal outlet is the pressure outlet, the two sides are symmetrical surfaces, and the hull surface is non-penetrable wall surface.

Fig. 8. Side view along the ship hull direction for the C11 container ship model.

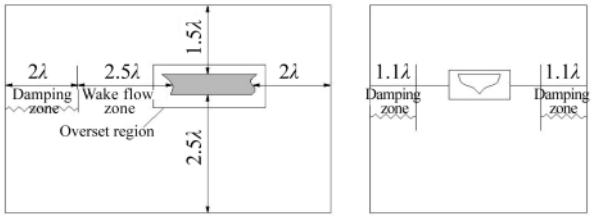

Fig. 9. Size of the computational fluid domain and damping zone.

4.5 Application of the overset mesh and mesh sensitivity analysis

To facilitate the large amplitude ship motions during the parametric rolling, the overset mesh method is used. The selection of overset region not only affects the number of grids in the computational domain, but also affects the computation of the overlapping boundary interpolation. Through our trial and error attempts, in the overset region, the width is 2.4 m and the boundaries from the bow and stern are 1 m, respectively, and the upward/downward boundaries from the calm water surface are 0.8 m and 1.2 m, respectively. The details can be found in Ge (2017).

The mesh setting around the ship hull in the overset region follows the meshing strategy when the free roll decay of the same ship model is performed using the overset grid method (Ma et al., 2017). The number of mesh around the bow, stern and bilge keel region is increased to study the convergence of the total number of mesh on the free decay roll motions in calm water.

For the mesh in the background mesh region, the meshing strategy has been presented in Section 4.2 of this paper. Both the upper and lower grids of the flow field from the calm water surface in the overlap region have the same size as the grids of the free surface in the background region.

By combining the meshing experience in the free roll decay simulation and wave generation tests, the mesh convergence test for the parametric rolling is performed for one wave condition, namely, when the wave steepness is 0.01 and the ship forward speed is Fn=0.05. The mesh close to the free surface is similar to the mesh strategy for the purpose of good wave quality setting in Section 4.2. The mesh size around the hull surface and nearby in the fluid are adjusted to have the intensity from relatively coarse setting to relatively finer setting; the mesh sizes on the hull surface are about 12.5, 9, and 6.25 mm, respectively; the total numbers of mesh are 3.74×10^6, 5.93×10^6, and 9.02×10^6, respectively.

Fig. 10 presents the parametric rolling for different numbers of meshes during the mesh convergence analysis. It is seen that the increase in the number of mesh has a quite

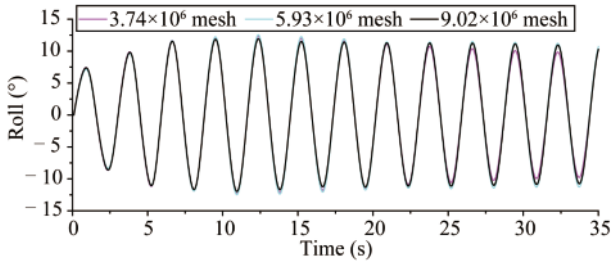

Fig. 10. Comparison of the parametric rolling response under different numbers of mesh.

small influence on the final steady parametric rolling. The number of mesh of 5.93×10^6 is proper for the numerical simulation of the parametric rolling in waves. In the following calculations, the meshing strategy is similar to this case; the exact mesh number is adjusted to have a good wave generation quality setting as discussed in Section 4.2.

The numerical calculations are done on a high-performance server. The parallel computation is run in two clusters with 40 cores in total. It takes about 5 CPU hours for 1 second real time simulation on an average.

5 Results and Discussion

5.1 Numerical simulation of the parametric rolling for the 11.5 m draft ship model under wave steepness of 0.03 and four forward speeds

Although the parametric rolling could develop rapidly once it occurs, the ship tends to encounter quite a few cycles of the wave excitation before reaching significant parametric rolling. As shown by the parametric rolling experiments in regular waves conducted by Zhao (2012), the initial roll angle has no effect on the final amplitude of the parametric rolling. To speed up the process of the parametric rolling and reduce the calculation time, the rolling angular velocity of 0.25 rad /s is exerted on the ship at the initial time moment.

During the course of the physical model tests of the ship, the ship model is free running and has 6-degree-of-freedom motion in waves. In view of the fact that the influence of the surge motion on the parametric rolling is negligible (Lu et al., 2017), the surge motion has been constrained in the following simulations. The remaining 5-degree-of-freedom of the ship motions are kept free.

Figs. 11–14 show the rolling and pitch time histories for the 11.5 m draft case and four different Froude numbers: Fn=0.0, 0.05, 0.1 and 0.15. The incident wave steepness is 0.03. In the comparison, the results from the potential flow theory of the nonlinear strip theory are also presented. As for the parametric rolling motions, it can be observed that both the nonlinear strip theory and CFD computations present quite good predictions on the parametric rolling amplitude; the numerical accuracy from the CFD results is generally better, especially for the case of Fn=0.15. As for the pitch motions, both the nonlinear strip theory and the CFD computations give larger predictions compared with the experimental data; the CFD results generally have better numerical accuracy. It is also observed from Figs. 11–14 that, under the same initial conditions, the higher the ship forward speed is, the more wave periods are encountered for the ship model before the parametric rolling starts.

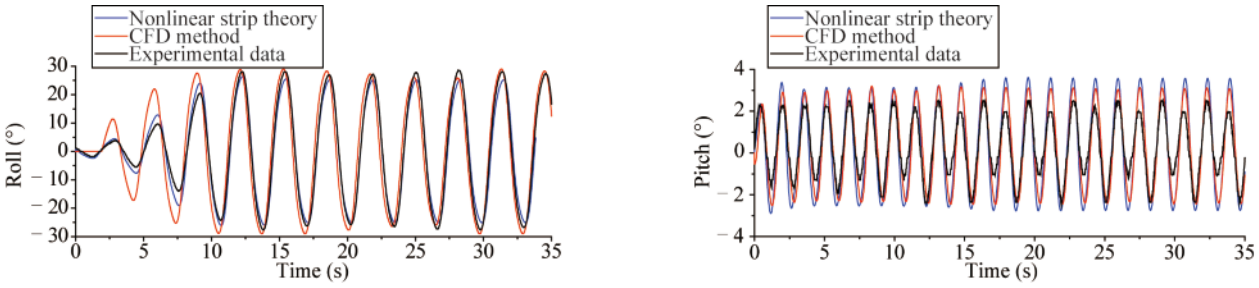

Fig. 11. Comparison of C11 container ship's rolling and pitching motions (Fn=0.0, H/λ=0.03).

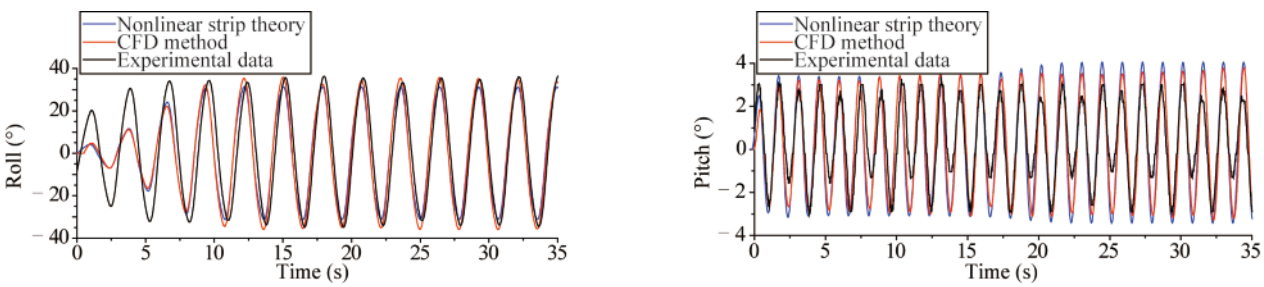

Fig. 12. Comparison of C11 container ship's rolling and pitching motions (Fn=0.05, H/λ=0.03).

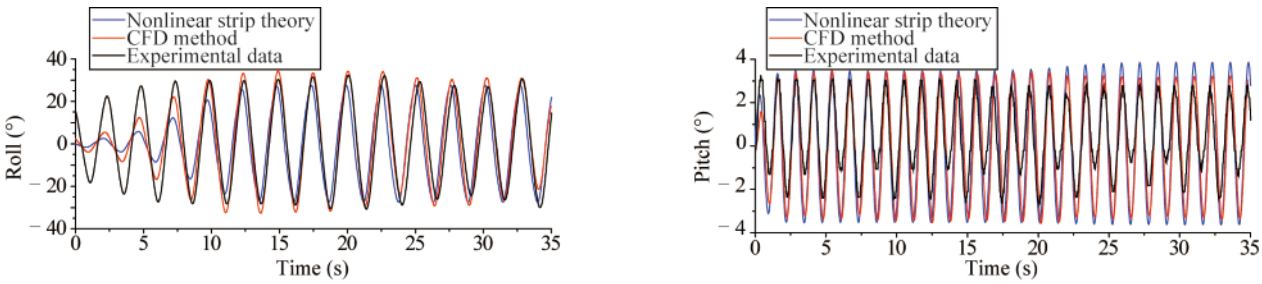

Fig. 13. Comparison of the roll and pitch motions of the C11 container ship in the time domain (Fn=0.1, H/λ=0.03).

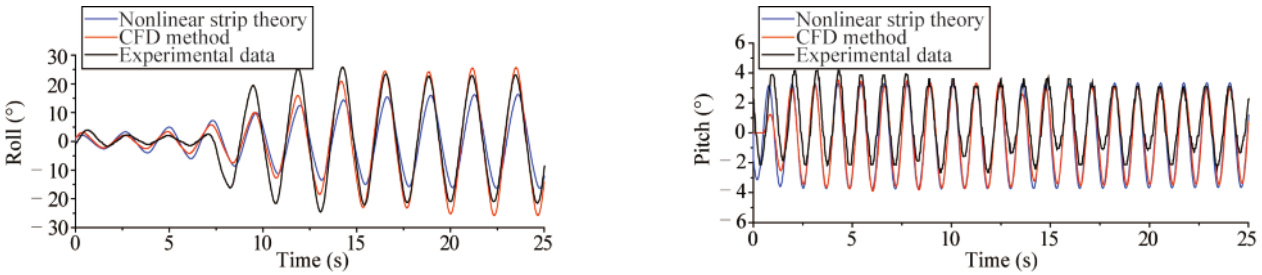

Fig. 14. Comparison of the roll and pitch motions of the C11 container ship in the time domain (Fn=0.15, H/λ=0.03).

5.2 Parametric rolling simulation for the 11.8 m draft ship model with relatively large wave steepness

In Fig. 5, the experimental parametric rolling amplitude for the C11 ship is given for a number of wave amplitudes. It is shown that the roll amplitude decreases at certain wave amplitudes. The reason for this phenomenon was given by Neves and Rodríguez (2007). In their analysis, they demonstrated that the strong coupling of the vertical motions in waves influences the dynamics of the parametric rolling. In the study of Hu et al. (2017), they attempted to simulate the parametric rolling at larger wave amplitudes for Fn=0.05 case using the nonlinear strip theory, and they observed that the experimental data are underestimated. The possible reason for this was analyzed. In the present study, the related reasons are explored by use of the current viscous RANS solver.

Figs. 15–18 show the motion responses for different wave steepness and for the 11.8 m draft and Froude number

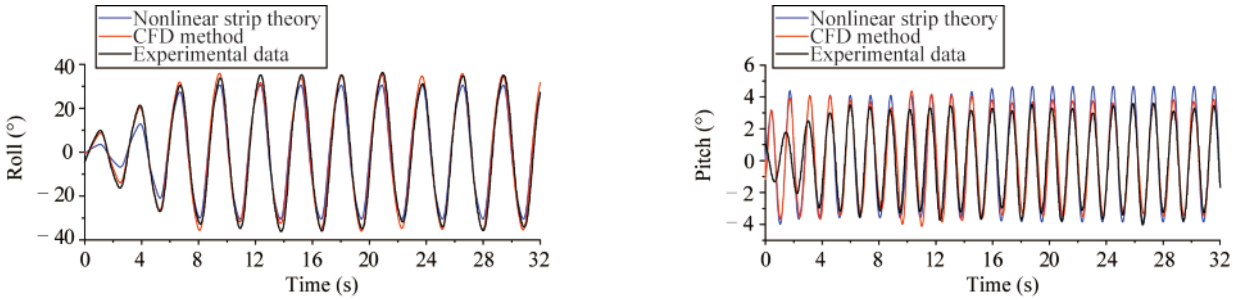

Fig. 15. Comparison of the motion response of Model 2 under the wave steepness of 0.04 (Fn=0.05).

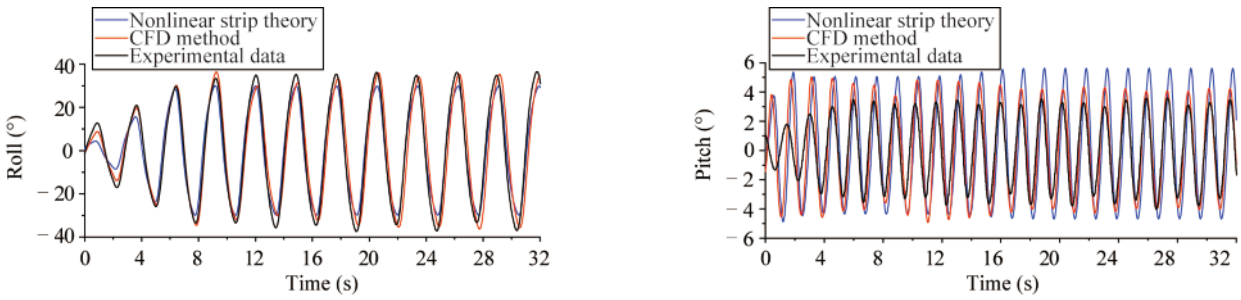

Fig. 16. Comparison of the motion response of Model 2 under the wave steepness of 0.05 (Fn=0.05).

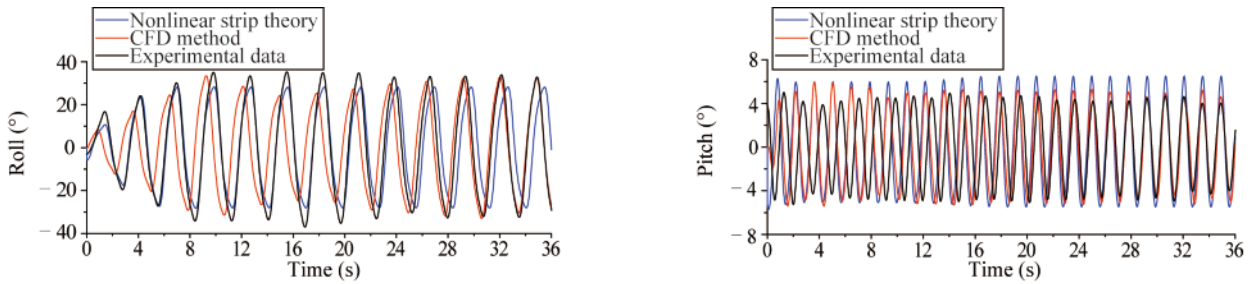

Fig. 17. Comparison of the motion response of Model 2 under the wave steepness of 0.06 (*Fn*=0.05).

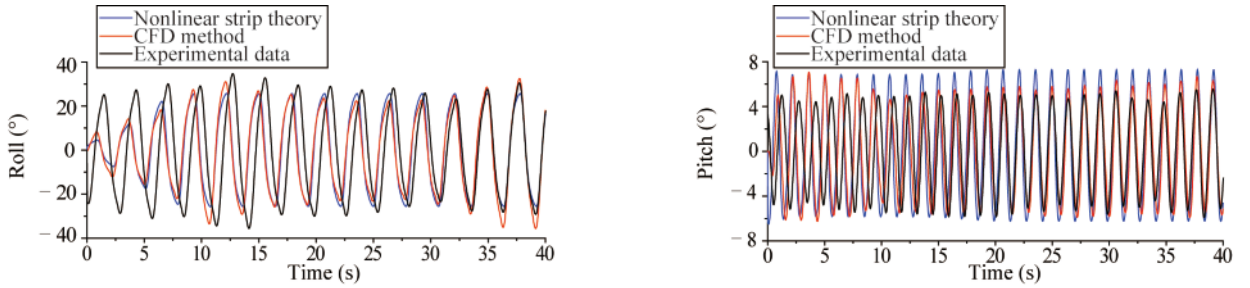

Fig. 18. Comparison of the motion response of Model 2 under the wave steepness of 0.07 (*Fn*=0.05).

of 0.05. As can be seen from these results, when the wave steepness is 0.04, the ship's roll motions from the nonlinear strip theory and CFD method have the same numerical accuracies, while the pitch motions obtained by the CFD computations are evidently better than those of the nonlinear strip theory predictions. At the wave steepness of 0.05, the parametric roll motions from both numerical results agree quite well with the experimental data, while the pitch motions from the CFD method look better. At the wave steepness of 0.06 and 0.07, the numerical simulations for the parametric rolling from the CFD method continue for longer encounter periods before reaching a steady amplitude. The final roll motions from the CFD method agree better with the experimental data. As for the pitch motions, the CFD results have a good agreement with those of the experiments, while the nonlinear strip theory results overestimate the measured value.

Fig. 19 presents the steady parametric rolling amplitude comparison at relatively larger incident wave steepness. It should be noted that at the ship forward speed of *Fn*=0.05, the encounter frequency of the ship is close to twice the ship roll natural frequency, and the ship experiences relatively significant parametric rolling motions. As can be seen from the results, with an increase in the steepness, the amplitude of the roll does not increase significantly. At the wave steepness of 0.05, the parametric rolling motion reaches the maximum. The amplitude of the parametric rolling obtained by the nonlinear strip theory evidently underestimates the measured value for the wave steepnesses of 0.06 and 0.07. On the other hand, the numerical simulations obtained by the CFD method present closer results to the

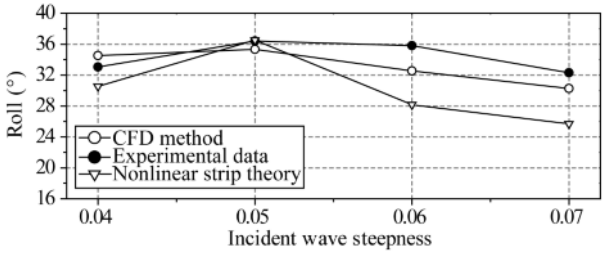

Fig. 19. Comparison of the steady roll amplitude of large wave steepness for Model 2 (*Fn*=0.05).

measured data than those predicted by the nonlinear strip theory.

The reasons for the better numerical accuracy obtained by the CFD results can be analyzed by the following respects. The first one is a better model of the restoring moment in waves. As discussed by Lu et al. (2017), the restoring moment variations have two components. One is the variation of the hydrostatic rolling moment due to the vertical ship motion in waves, which can be calculated by integrating the incident wave pressure and hydrostatic pressure under the instantaneous wetted hull surface. Another component is the hydrodynamic rolling moment due to the coupling effect of the radiation forces and diffraction forces caused by the vertical ship motions at a certain rolling angle. The consideration of the restoring moment from the nonlinear radiation force and diffraction force contributions generally produces larger restoring variation and parametric rolling as shown by Lu et al. (2017). In the current CFD analysis, both components of the restoring moment variations are considered, while only the hydrostatic compon-

ent is considered for the potential-flow based the nonlinear strip theory. This is the reason for better agreement of the parametric rolling for the relatively larger amplitudes of 0.06 and 0.07. It can be concluded that the hydrodynamic component of the restoring moment becomes more important when the rolling angle is relatively large at higher incident wave steepnesses. In the potential-flow model, it is necessary to consider the contribution of the restoring moment from the radiation/diffraction forces at relatively large wave steepnesses if better results are needed. The second one is the better modeling of the ship roll damping. It is commonly acknowledged that the roll damping is quite important in quantitatively predicting the steady parametric amplitude (Schumacher et al., 2016). The rolling damping model for relatively large amplitudes is still an open issue. In the nonlinear strip theory, the free decay rolling curve at certain initial amplitude is used to obtain the roll damping and used at the numerical simulation of the parametric rolling. As discussed in Hu et al. (2017), the roll damping coefficients were used to predict the parametric rolling amplitude at higher roll amplitudes, whose damping was possibly overestimated for large roll amplitudes and causes the parametric rolling amplitude to be smaller than the experimental data. On the other hand, the roll damping is consistently solved together with the nonlinear ship motions by the CFD model which provides more accurate estimation of the ship roll damping and ship roll motions thereafter.

6 Further discussion and conclusions

In this paper, both the experimental and numerical studies are conducted to investigate the ship parametric rolling for the C11 containership in regular waves. The following conclusions can be drawn.

(1) The parametric rolling for the ship models with different drafts is compared, and the steady rolling amplitude for the smaller draft is generally found to be larger. It is found that different restoring moments contribute to the finding of different steady parametric rolling amplitudes for the ship model with two different drafts. The sensitivity of the ship draft at the aft stations to the inception of the parametric rolling is significant, and this provides important information on reducing the parametric rolling from the ship design and operation respective

(2) In this paper, the numerical calculation of the parametric rolling in regular head seas is performed using the viscous flow CFD method. The RANS method has been successfully applied to predict the parametric rolling response in regular waves. Via the current study, it is concluded that the CFD method can give satisfactory numerical results by the proper mesh setting and suitable dynamic mesh method. At the current stage, the CFD computations are still very time consuming and cannot replace the potential-flow model. However, it can be a beneficial supplement to the potential-flow model and be helpful in investigating the application range and the limitation of the potential-flow model. As the computers become much faster, computational efficiency will not obviously be an issue but computational accuracy will still be an issue due to difficulties in the numerical methods used as well as in turbulence modeling.

(3) The parametric ship rolling for the C11 containership with different drafts is estimated with both the potential-flow based the nonlinear strip theory and CFD method. At smaller wave steepness of 0.03, it is found that both the potential-flow and CFD methods provide quite good predictions of the steady amplitude of the parametric rolling. While at larger wave steepness, especially for 0.05–0.07, the numerical results obtained by the CFD method evidently gives better predictions. It is concluded that it is necessary to consider the contribution of the radiation/diffraction force on the hydrodynamic restoring moment at larger wave steepnesses in the case of the potential-flow model if better numerical accuracy is desired.

(4) In this paper, the effect of the incident wave amplitude (wave steepness) at certain frequency on the steady parametric rolling is investigated by both the experimental and numerical methods. It is found that the amplitude of the ship parametric rolling no longer increases with the increase in the wave steepness under certain incident wave amplitudes. The results provide physical evidence and confirm the related analytical analysis of the limits of the stability about the effect of the nonlinear restoring moment, which originates from the third-order coupling of the vertical motions on the parametric rolling excitation in waves.

Acknowledgements

In this work, part of the experimental study for the C11 containership is jointly carried out by CSSRC and HEU. The model test data of the parametric rolling is provided by Prof. Gu M. and Dr. Lu J. from China Ship Scientific Research Center (CSSRC). Their help is gratefully acknowledged.

References

Bulian, G., 2006. *Development of Analytical Nonlinear Models for Parametric Roll and Hydrostatic Restoring Variations in Regular and Irregular Waves*, Ph. D. Thesis, University of Trieste, Trieste, Italy.

Bulian, G., Francescutto, A., Umeda, N. and Hashimoto, H., 2008. Qualitative and quantitative characteristics of parametric ship rolling in random waves in the light of physical model experiments, *Ocean Engineering*, 35(17–18), 1661–1675.

Castiglione, T., Stern, F., Bova, S. and Kandasamy, M., 2011. Numerical investigation of the seakeeping behavior of a catamaran advancing in regular head waves, *Ocean Engineering*, 38(16), 1806–1822.

Galbraith, A. and Boulougouris, E., 2015. Parametric rolling of the tumblehome hull using CFD, *Proceedings of the 12th International Conference on the Stability of Ships and Ocean Vehicles*, University of Strathclyde, Glasgow, UK, pp. 535–543.

Ge, W.P., 2017. *An Investigation of Ship Parametric Rolling Simulation in Regular Wave Based on the CFD Method*, MSc. Thesis, Har-

bin Engineering University, Harbin, China. (in Chinese)

Gu, M., Lu, J. and Wang, T.H., 2014. Experimental and numerical study on roll restoring variation using the C11 containership, *Proceedings of the 14th International Ship Stability Workshop*, Kuala Lumpur, Malaysia, pp. 126–132.

Hashimoto, H. and Umeda, N., 2004. Nonlinear analysis of parametric rolling in longitudinal and quartering seas with realistic modeling of roll-restoring moment, *Journal of Marine Science and Technology*, 9(3), 117–126.

Hu, K.Y., Wang, R., Ma, S., Duan, W.Y., Xu, W.H. and Deng, R., 2017. Numerical modelling and study of parametric rolling for C11 containership in regular head seas using consistent strip theory, *Brodogradnja*, 68(3), 135–156.

International Maritime Organization, 2015. SDC 2/WP.4. 2nd Session. Development of second generation intact stability criteria, Development of amendments to part B of the 2008 IS code on towing and anchor handling operations.

International Maritime Organization, 2016. SDC 3/WP.5, 3rd Session. Finalization of second generation intact stability criteria, Amendments to part B of the 2008 IS code on towing, lifting and anchor handling operations.

Kim, T.Y., Kim, Y. and Park, D.M., 2011. Study on the occurrence of parametric roll in bichromatic Waves, *Proceedings of the 26th International Workshop on Water Waves and Floating Bodies*, Athens, Greece.

Liu, S.K. and Papanikolaou, A., 2016. Prediction of parametric rolling of ships in single frequency regular and triple frequency group waves, *Ocean Engineering*, 120, 274–280.

Lu, J., Gu, M., Ma, K. and Huang, W.G., 2012a. A study on parametric rolling in irregular waves, *Journal of Ship Mechanics*, 16(8), 893–900. (in Chinese)

Lu, J., Gu, M. and Umeda, N., 2012b. Numerical approaches on parametric rolling in head seas, *Proceedings of the 10th International Conference on Hydrodynamics*, St. Petersburg, Russia.

Lu, J., Gu, M. and Umeda, N., 2016. A study on the effect of parametric roll on added resistance in regular head seas, *Ocean Engineering*, 122, 288–292.

Lu, J., Gu, M. and Umeda, N., 2017. Experimental and numerical study on several crucial elements for predicting parametric roll in regular head seas, *Journal of Marine Science and Technology*, 22(1), 25–37.

Ma, S., Ge, W.P., Duan, W.Y. and Liu, H.X., 2017. Simulation of free decay roll for C11 container ship based on overset gird, *Journal of Huazhong University of Science and Technology* (*Nature Science Edition*), 45(5), 34–39. (in Chinese)

Ma, S., Wang, R., Zhang, J., Duan, W.Y., Ertekin, R.C. and Chen, X.B., 2016. Consistent formulation of ship motions in time-domain simulations by use of the results of the strip theory, *Ship Technology Research*, 63(3), 146–158.

Neves, M.A.S. and Rodríguez, C.A., 2006. On unstable ship motions resulting from strong non-linear coupling, *Ocean Engineering*, 33(14–15), 1853–1883.

Neves, M.A.S. and Rodríguez, C.A., 2007. Influence of non-linearities on the limits of stability of ships rolling in head seas, *Ocean Engineering*, 34(11–12), 1618–1630.

Schumacher, A., Ribeiro, S.S. and Guedes Soares, C., 2016. Experimental and numerical study of a containership under parametric rolling conditions in waves, *Ocean Engineering*, 124, 385–403.

Simonsen, C.D., Otzen, J.F., Joncquez, S. and Stern, F., 2013. EFD and CFD for KCS heaving and pitching in regular head waves, *Journal of Marine Science and Technology*, 18(4), 435–459.

Tezdogan, T., Demirel, Y.K., Kellett, P., Khorasanchi, M., Incecik, A. and Turan, O., 2015. Full-scale unsteady RANS CFD simulations of ship behaviour and performance in head seas due to slow steaming, *Ocean Engineering*, 97, 186–206.

Thomas, G., Duffy, J., Lilienthal, T., Watts, R. and Gehling, R., 2008. Parametric rolling in head seas–an Australian perspective, *Proceedings of the 6th Osaka Colloquium on Seakeeping and Stability of Ships*, Osaka University, Osaka, Japan, pp. 312–317.

Zhao, C.H., 2012. *Theoretical and Experimental Research on Parametric Rolling of A Container Ship*, MSc. Thesis, Harbin Engineering University, Harbin, China. (in Chinese)

Zhou, Y.H., Ma, N., Lu, J. and Gu, M., 2016. A study of hybrid prediction method for ship parametric rolling, *Journal of Hydrodynamics*, *Ser. B*, 28(4), 617–628.